

Hyperon Physics Results from SELEX¹

The SELEX Collaboration

I. Eschrich^{i,2}, N. Akchurin^q, V. A. Andreev^k, A.G. Atamantchouk^k, M. Aykac^q, M.Y. Balatz^h, N.F. Bondar^k, A. Bravar^v, M. Chensheng^g, P.S. Cooper^e, L.J. Dauwe^r, G.V. Davidenko^h, U. Derschⁱ, A.G. Dolgolenko^h, D. Dreossi^v, G.B. Dzyubenko^h, R. Edelstein^c, A.M.F. Endler^d, J. Engelfried^{e,m}, C. Escobar^{u,3}, A.V. Evdokimov^h, T. Ferbel^s, I.S. Filimonov^{j,4}, F. Garcia^u, M. Gaspero^t, S. Gerzon^l, I. Giller^l, G. Ginther^s, V.L. Golovtsov^k, Y.M. Goncharenko^f, E. Gottschalk^{c,e}, P. Gouffon^u, O.A. Grachov^{f,5}, E. Gülmez^b, C. Hammer^s, M. Iori^t, S.Y. Jun^c, A.D. Kamenski^h, H. Kangling^g, M. Kaya^q, C. Kenney^p, J. Kilmer^e, V.T. Kim^k, L.M. Kochenda^k, K. Königsman^{i,6}, I. Konorov^{i,7}, A.A. Kozhevnikov^f, A.G. Krivshich^k, H. Krügerⁱ, M.A. Kubantsev^h, V.P. Kubarovsky^f, A.I. Kulyavtsev^{f,c}, N.P. Kuropatkin^k, V.F. Kurshetsov^f, A. Kushnirenko^c, S. Kwan^e, J. Lach^e, A. Lamberto^v, L.G. Landsberg^f, I. Larin^h, E.M. Leikin^j, M. Luksysⁿ, T. Lungov^{u,8}, D. Magarrel^q, V.P. Maleev^k, D. Mao^{c,9}, S. Masciocchi^{i,10}, P. Mathew^{c,11}, M. Mattson^c, V. Matveev^h, E. McCliment^q, S.L. McKenna^o, M.A. Moinester^l, V.V. Molchanov^f, A. Morelos^m, V.A. Mukhin^f, K. Nelson^q, A.V. Nemitkin^j, P.V. Neouistroev^k, C. Newsom^q, A.P. Nilov^h, S.B. Nurushev^f, A. Ocherashvili^l, G. Oleynik^{e,12}, Y. Onel^q, E. Ozel^q, S. Ozkorucuklu^q, S. Parker^p, S. Patrichev^k, A. Penzo^v, P. Pogodin^q, B. Povhⁱ, M. Procario^c, V.A. Prutsko^h, E. Ramberg^e, G.F. Rappazzo^v, B. V. Razmyslovich^k, V. Rud^j, J. Russ^c, P. Schiavon^v, V.K. Semyatchkin^h, Z. Shuchen^g, J. Simonⁱ, A.I. Sitnikov^h, D. Skow^e, P. Slattey^s, V.J. Smith^{o,13}, M. Srivastava^u, V. Steiner^l, V. Stepanov^k, L. Stutte^e, M. Svoiski^k, N.K. Terentyev^{11,3}, G.P. Thomas^a, L.N. Uvarov^k, A.N. Vasiliev^f, D.V. Vavilov^f, V.S. Verebryusov^h, V.A. Victorov^f,

¹) Presented at the Workshop on Heavy Quarks at Fixed Target, Fermilab, Oct. 10-12, 1998

²) Now at Imperial College, London SW7 2BZ, U.K.

³) Present address: Instituto de Fisica da Universidade Estadual de Campinas, UNICAMP, SP, Brazil.

⁴) deceased

⁵) Present address: Dept. of Physics, Wayne State University, Detroit, MI 48201, U.S.A.

⁶) Present address: Universität Freiburg, 79104 Freiburg, Germany

⁷) Present address: Physik-Department, Technische Universität München, 85748 Garching, Germany

⁸) Current Address: Instituto de Fisica Teorica da Universidade Estadual Paulista, São Paulo, Brazil

⁹) Present address: Lucent Technologies, Naperville, IL

¹⁰) Now at Max-Planck-Institut für Physik, München, Germany

¹¹) Present address: Motorola Inc., Schaumburg, IL

¹²) Present address: Lucent Technologies, Naperville, IL

¹³) Generous support of Carnegie-Mellon University is gratefully acknowledged.

V.E. Vishnyakov^h, A.A. Vorobyov^k, K. Vorwalter^{i,14}, Z. Wenheng^g, J. You^c,
L. Yunshan^g, M. Zhenlin^g, L. Zhigang^g, M. Zielinski^s, R. Zukanovich Funchal^u

^a Ball State University, Muncie, IN 47306, U.S.A.

^b Bogazici University, Bebek 80815 Istanbul, Turkey

^c Carnegie-Mellon University, Pittsburgh, PA 15213, U.S.A.

^d Centro Brasileiro de Pesquisas Físicas, Rio de Janeiro, Brazil

^e Fermilab, Batavia, IL 60510, U.S.A.

^f Institute for High Energy Physics, Protvino, Russia

^g Institute of High Energy Physics, Beijing, PR China

^h Institute of Theoretical and Experimental Physics, Moscow, Russia

ⁱ Max-Planck-Institut für Kernphysik, 69117 Heidelberg, Germany

^j Moscow State University, Moscow, Russia

^k Petersburg Nuclear Physics Institute, St. Petersburg, Russia

^l Tel Aviv University, 69978 Ramat Aviv, Israel

^m Universidad Autonoma de San Luis Potosí, San Luis Potosí, Mexico

ⁿ Universidade Federal da Paraíba, Paraíba, Brazil

^o University of Bristol, Bristol BS8 1TL, United Kingdom

^p University of Hawaii, Honolulu, HI 96822, U.S.A.

^q University of Iowa, Iowa City, Iowa 52242, U.S.A.

^r University of Michigan-Flint, Flint, MI 48502, U.S.A.

^s University of Rochester, Rochester, NY 14627, U.S.A.

^t University of Rome "La Sapienza" and INFN, Rome, Italy

^u University of São Paulo, São Paulo, Brazil

^v University of Trieste and INFN, Trieste, Italy

Abstract. In parallel to charm hadroproduction the experiment SELEX (E781) at Fermilab is pursuing a rich hyperon physics program. SELEX employs a 600 GeV/c beam consisting of 50 % Σ^- and π^- each. The three-stage magnetic spectrometer covering $0.1 \leq x_F \leq 1.0$ features a high-precision silicon vertex system, broad-coverage particle identification using TRD and RICH, and a three-stage lead glass photon calorimeter. First results for the Σ^- charge radius, total Σ^- - nucleon cross sections, and a new upper limit for the radiative width of the $\Sigma(1385)^-$ are presented.

I INTRODUCTION

In parallel to charm hadroproduction the hyperon beam experiment SELEX (E781) at Fermilab is pursuing a rich hyperon physics program. One year after the end of the 1997 fixed target run, first results are available.

The apparatus has been described already elsewhere in these proceedings [1]. Ongoing projects include the measurement of hyperon charge radii by hyperon-electron elastic scattering, the Σ^- -proton total cross section, Primakoff production

¹⁴⁾ *Present address: Deutsche Bank AG, 65760 Eschborn, Germany*

of hyperon resonances, Σ^+ production polarization, and the search for exotic particles produced by hyperon-induced reactions to name a few examples. The hyperon physics program is complemented by analysis of the data taken with π^- and proton beams, which has also yielded first results [2].

II CHARGE RADII

Hadrons as we understand them today are composite systems which we characterize by their static properties. One static property which reflects the phenomenon unique to hadrons – quark confinement – is the size of the particle.

Elastic scattering of an electron off a charged hadron is modified from a point interaction by the form factor $F(Q^2)$ where Q^2 is the four-momentum transfer squared. At zero momentum transfer the mean squared charge radius is related to the slope of the form factor by

$$\langle r^2 \rangle = -6\hbar^2 \left. \frac{dF(Q^2)}{dQ^2} \right|_{Q^2=0}.$$

Charge radii are known only for five different hadrons so far. The fact that the K^- radius has been found to be smaller than that of the π^- by $\sim 0.1 \text{ fm}^2$ suggests that the size of a hadron is related to the flavor composition of its constituent quarks. There is supporting evidence from a study of strong interaction radii [3] which finds that replacing an *up* or *down* quark by a *strange* quark in a baryon decreases its radius by approximately 0.08 fm^2 . Consequently the Σ^- radius should be smaller than the proton radius, and larger than the Ξ^- . The definition of a strong-interaction radius, however, is model-dependent. The significance of the above observation is therefore limited unless validated by a systematic study of hyperon charge radii.

For hadron-electron elastic scattering, two hits in the negative and none in the positive half of a hodoscope downstream of the second magnet in coincidence with a multiplicity of two in a set of scintillation counters 3 cm downstream of the target constituted a valid trigger condition. The typical trigger rate at this level was 3000 per 20-second spill at a beam rate of 10^7 particles per spill. An online filter performed a preliminary track reconstruction in the M2 spectrometer. Requiring at least one track with negative and none with positive slope together with other conditions crucial to a complete reconstruction reduced this sample by a factor of 1:1.7.

In the 1997 run SELEX has recorded 215 million candidates for hadron-electron scattering with the Σ^-/π^- -beam. In preparation for a first analysis with the software tools available at that time the negative-beam sample was stripped to 10 % of its original size by cutting on an electron signature, unambiguous identification of the beam particle, and a two-negative-track event topology. A second-stage strip required a two-prong vertex, again reducing the sample by a factor of 10.

Out of the stripped data sample described above, 12,000 Σ^- -electron and 26,000 π^- -electron elastic scattering events were extracted. For each event, the incoming and outgoing tracks in the vertex were required to be coplanar. Particle identification for the two outgoing tracks was performed by combining information from the transition radiation detectors with kinematic constraints. Events with ambiguous particle identification were discarded. For Σ^- , decays upstream of the M2 chambers

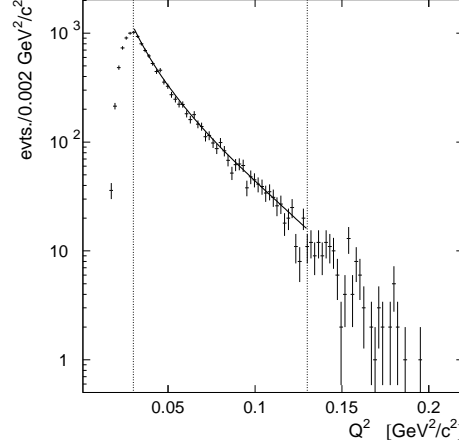


FIGURE 1. Q^2 distribution of Σ^- -electron scattering events. Vertical lines indicate the region accepted for fitting.

were rejected by requiring the scattered beam particle to have at least 60 % of the incoming beam particle's momentum. Finally, electron momentum and scattering angle had to match their expected kinematic relation to better than 10 %.

The charge radii were determined by fitting the differential cross section with an assumed radius as the single parameter to the observed distribution of the four-momentum transfer squared Q^2 (Fig. 1). Since the shape of the Q^2 -distribution yields the radius no absolute normalization is needed. In this first analysis, Q^2 was calculated from the beam momentum and the scattering angle of the electron. From Monte Carlo studies the Q^2 resolution was estimated to be 1.5 %. Preliminary acceptance studies were performed using generated elastic scattering events embedded in real data. The geometrical and reconstruction-dependent acceptance was modeled and a preliminary evaluation of the trigger efficiency performed.

For the Σ^- data, a Q^2 region with flat acceptance was chosen for fitting the radius. For the π^- data, an acceptance correction was applied. Each event was normalized to its individual beam momentum to eliminate effects of the beam momentum spread. An unbinned maximum likelihood fit using dipole electric and magnetic form factors for the Σ^- yields a mean squared charge radius of

$$\langle r^2 \rangle_{\Sigma^-} = 0.60 \pm 0.08 \text{ (stat.)} \pm 0.08 \text{ (syst.) fm}^2$$

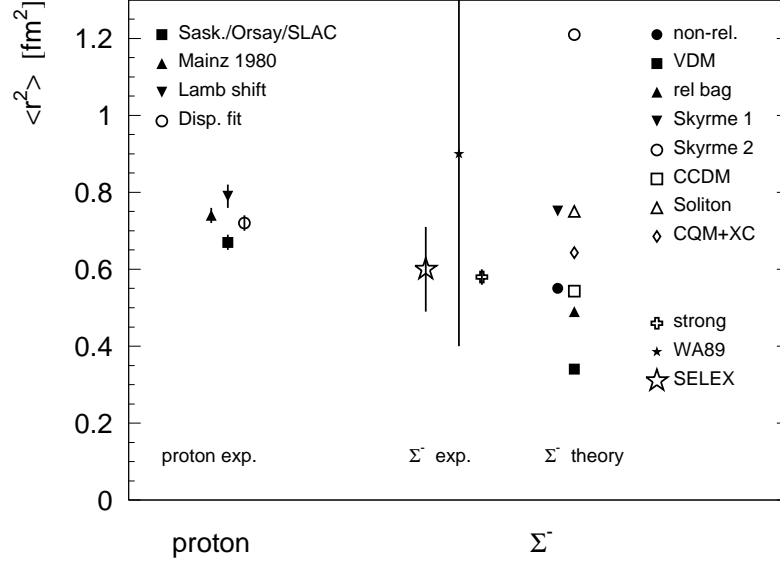


FIGURE 2. The Σ^- charge radius compared to various results for the proton radius (left): *Sask./Orsay/SLAC* [10,11], *Mainz* [9], *dispersion-theoretical fit* to all of above [12], and *Lamb shift* [13]. – Experimental results (center): *SELEX*: this measurement, *WA89*: WA89 result [5], *strong*: strong interaction radius [3]. – The predictions for Σ^- refer to the following models: *non-rel.*: non-relativistic quark model, *VDM*: vector dominance model, *rel bag*: relativistic bag model (all three values from [3]), *Skyrme 1*: Skyrme model [14], *Skyrme 2*: Skyrme model [15], *CCDM*: Chiral color dielectric model [16], *Soliton*: Soliton model [17], *CQM+XC*: Chiral constituent quark model including exchange currents [18].

in the Q^2 region of $0.03 \leq Q^2 \leq 0.16 \text{ GeV}^2/c^2$ (7,800 events) [4]. This result is well inside the limits determined by the WA89 collaboration [5], $0.4 \text{ fm}^2 \leq \langle r^2 \rangle_{\Sigma^-} \leq 1.4 \text{ fm}^2$ (Fig. 2).

For the negative pion, a monopole electric form factor is used. We find

$$\langle r^2 \rangle_{\pi} = 0.45 \pm 0.03 \text{ (stat.)} \pm 0.07 \text{ (syst.) fm}^2,$$

where $0.03 \leq Q^2 \leq 0.20 \text{ GeV}^2/c^2$. (12,000 events) [6]. This result is in excellent agreement with the so far best direct measurement [7] of $\langle r^2 \rangle_{\pi} = 0.44 \pm 0.01 \text{ fm}^2$ as well as a recent calculation which takes into account form factor measurements in both space-like and time-like regions [8]: $\langle r^2 \rangle_{\pi} = 0.463 \pm 0.005 \text{ fm}^2$.

Major contributions to the systematic error come from the Q^2 resolution, uncertainties in the corrections for trigger efficiency, and beam contamination by other particles, particularly Ξ^- . Significant improvement is expected for all of these when advanced reconstruction and simulation software is used to refine the data sample.

Q^2 will be determined from all kinematic variables and events with identified Σ^- decays accepted as well. We anticipate a statistical error of less than 10 % in the final analysis of the Σ^- radius.

III Σ^-p TOTAL CROSS SECTION

In general, the difference of total hadronic cross sections is ascribed to the difference in Regge residue functions, which are connected to hadronic radii, rather than to the Pomeron propagator. In the Landshoff-Donnachie [19] version of Regge theory the effective Pomeron intercept $\epsilon \approx (\alpha_P(0) - 1)$ and the effective Reggeon intercept $\eta \approx (\alpha_R(0) - 1)$ are assumed to be universal, i.e. the same for all hadrons, with $\epsilon \approx 0.08$ and $\eta \approx 0.47$.

Recent data from H1 and ZEUS on the proton structure function at small x and high Q^2 demonstrate, however, that the effective Pomeron intercept is higher for hadrons with smaller radii, up to $\epsilon = 0.4$ for high Q^2 [20]. There is further evidence for $\epsilon > 0.08$ from real exclusive photoproduction of heavy flavors. Data from HERA also show that the cross section of J/Ψ photoproduction rises by a factor of 6 from $\sqrt{s} = 10$ to 100 GeV [21,24].

This Q^2 dependence of the ϵ should have its counterpart in the ϵ dependence on the radii of the stable hyperons. The higher the quark mass, the smaller the interquark distance corresponding to the effective high Q^2 hadronic interaction.

The only available beams with flavors heavier than *up* or *down* are K^\pm and hyperon beams. Total cross sections of Σ^- and Ξ^- on protons and deuterons have been measured at beam energies between 19–137 GeV at CERN [22,27]. Analogous data at 600 GeV would provide a sensitive test of the Pomeron universality [23].

In the 1997 fixed target run SELEX has recorded 58 million events with Σ^-/π^- and 18 million with proton/ π^+ beams using a beam-only trigger. Beam particles were identified with a transition radiation detector. Corrections were applied to account for effects of Coulomb and Coulomb-nuclear interference as well as beam rate and contamination.

The total hadronic Σ^-p cross section at 600 GeV/ c beam momentum has been determined by the transmission method:

$$\sigma_{tot}(\Omega) := \frac{1}{\rho L} \lim_{\Omega \rightarrow 0} \log \left[\frac{F_0}{F_{tr}(\Omega)} \cdot \frac{E_{tr}(\Omega)}{E_0} \right].$$

Here, ρ and L are density and length of the target, and F_{tr}/F_0 and E_{tr}/E_0 the transmission ratios with and without target, respectively. Instead of a liquid hydrogen target SELEX had two alternative approaches:

- (1) C-CH₂ subtraction method. From the data sample taken with carbon and polyethylene targets the total Σ^- -proton cross section was calculated from

$$\sigma_{tot}(\Sigma^- p) = \frac{1}{2} \left[\sigma_{tot}(\Sigma^- CH_2) - \sigma_{tot}(\Sigma^- C) \right].$$

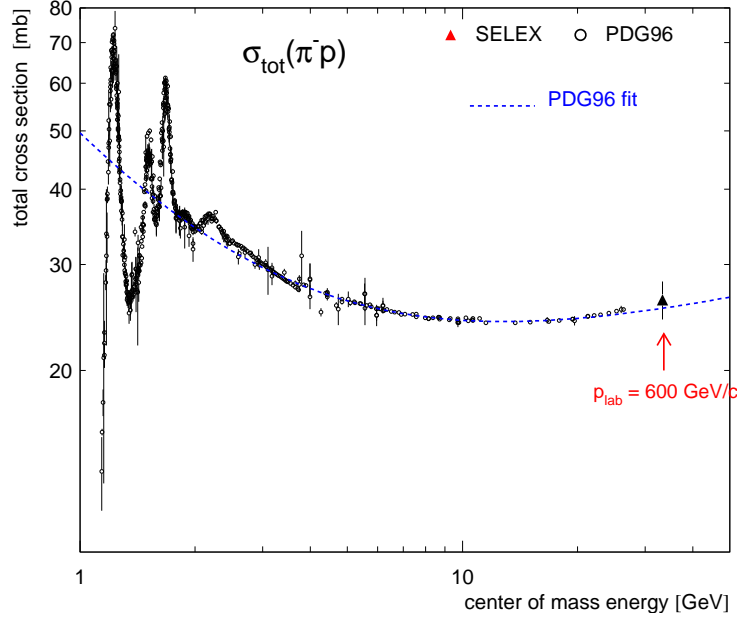


FIGURE 3. Compilation of world data on π^-p total cross sections with the preliminary SELEX result at 600 GeV/ c beam momentum.

This yields

$$\sigma_{tot}(\Sigma^- p) = 34.0 \pm 1.9 \text{ mb},$$

where statistical and systematic errors have been combined. As a cross check, an identical analysis was performed on the pion-proton data taken with these targets:

$$\sigma_{tot}(\pi^- p) = 26.2 \pm 1.9 \text{ mb}$$

A comparison to the current world data sample which only covers beam momenta up to 370 GeV/ c [26] finds our results to be following the general trend (Fig. 3).

- (2) $\sigma_{tot}(\Sigma^- p)$ was calculated from the ratio of proton-nucleus and Σ^- -nucleus cross sections. Here, we used Be and C targets. The Σ^- -nucleus cross sections for Be and C targets follow nicely the expected A -dependence of $\sigma_{tot}(XA) = \sigma_0 A^\alpha$, where $\alpha \simeq 0.77$ [25]. The Σ^- -proton cross section was calculated from the ratio $\sigma_{tot}(\Sigma^- A)/\sigma_{tot}(pA)$. Nuclear effects were accounted for by a model based on Glauber theory which included corrections for inelastic nuclear shadowing. This leads to the result of $\sigma_{tot}(\Sigma^- p) = 36.39 \pm 0.76 \text{ mb}$ (Be target, 635 GeV/ c average beam momentum) and $\sigma_{tot}(\Sigma^- p) = 36.13 \pm 0.42 \text{ mb}$ (C target, 595 GeV/ c).

The results are shown along with total $\Sigma^- p$ cross sections at lower energies in Fig. 4. A fit to these data points using the Donnachie-Landshoff parametrization

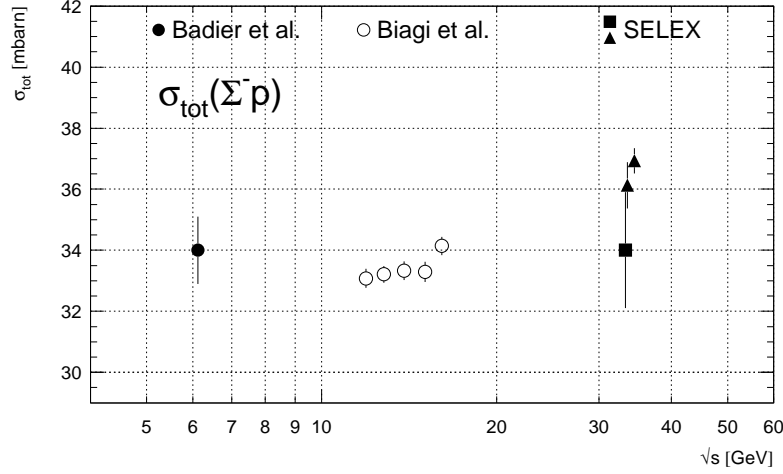


FIGURE 4. Total Σ^-p cross section at different center-of-mass energies. Low-energy data from Badier et al. [27] and WA42 (Biagi et al. [22]). SELEX results from C-CH₂ difference (square) and C and Be target Glauber calculations (triangles).

[26] yields $\epsilon = 0.098 \pm 0.019$ [25].

IV RADIATIVE WIDTH OF $\Sigma(1385)^-$

Radiative decay widths of hyperons constitute powerful tests for dynamical theories of hadronic systems. The expected value of the SU(3)-suppressed radiative width $\Gamma(\Sigma^{*-} \rightarrow \Sigma^- \gamma)$ in different models is predicted in the region of 1–10 keV and the SU(3)-allowed width $\Gamma(\Sigma^{*+} \rightarrow \Sigma^+ \gamma)$ in the range of 100–300 keV [28]. Unfortunately, the experimental situation is difficult due to small branching ratios on one hand and large background from hadronic decays on the other.

The production of a hadron resonance state in the nuclear Coulomb field (the Primakoff formalism), on the other hand, provides a relatively clean method for the determination of radiative widths.

At SELEX, the $\Sigma(1385)^-$ was produced from Σ^- using a lead target. The differential cross section for the Primakoff reaction

$$\Sigma^- + Z \rightarrow Z + \Sigma(1385)^-, \quad \Sigma(1385)^- \rightarrow \Lambda + \pi^-$$

can be written as a function of the four-momentum transfer squared t ,

$$\frac{d\sigma}{dt} = 8\pi\alpha Z^2 \frac{2J_{\Sigma^*} + 1}{2J_{\Sigma} + 1} \Gamma(\Sigma(1385)^- \rightarrow \Sigma^- \gamma) \left(\frac{m_{\Sigma^*}}{m_{\Sigma^*}^2 - m_{\Sigma}^2} \right)^3 \frac{t - t_{\min}}{t^2} |F(t)|^2,$$

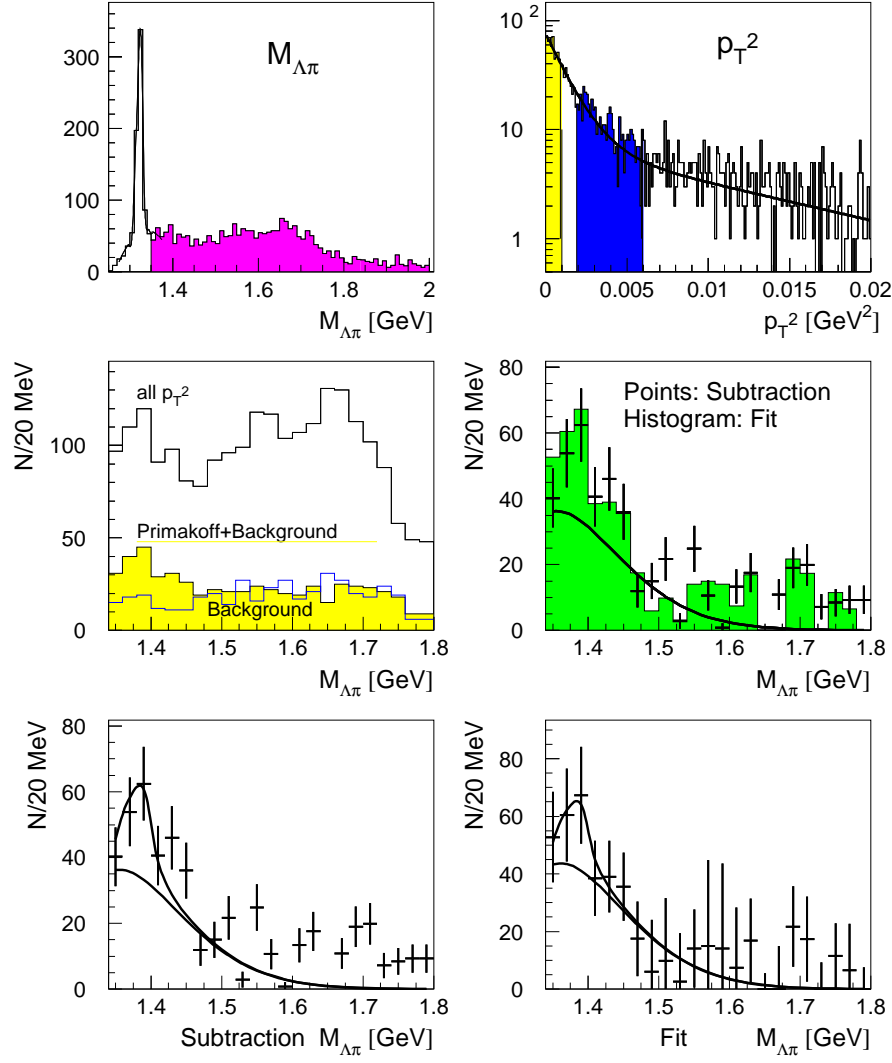


FIGURE 5. Transverse momentum squared and mass spectrum of the final state of $\Sigma^- + \text{Pb} \rightarrow \text{Pb} + (\pi^- + \Lambda)$, $\Lambda \rightarrow p + \pi^-$. Explanations in text (section IV).

where α is the fine structure constant, t_{min} the minimal momentum transfer squared, and m_{Σ^*} the mass of the final state. Z is the charge and $F(t)$ the electromagnetic form factor of the nucleus. The t -distribution for the Primakoff reaction has a pronounced forward peak at $t = 2t_{min}$.

The beam Σ^- was identified with a TRD. Elasticity of the reaction and less than 2 GeV of energy deposition in the first lead glass calorimeter were required. The observed $\Lambda\pi^-$ mass distribution is shown in Fig. 5 (upper left), with the peak from Ξ^- decays in the lead target clearly visible. The observed p_T^2 distribution (Fig. 5, upper right) was assumed to be the sum of coherent $\Lambda\pi$ and Primakoff production. From Monte Carlo simulation we found that both coherent and Primakoff p_T^2 distributions smeared by the experimental resolution can be described by double-exponential fits [30].

Two methods were used to estimate the $\Lambda\pi$ mass distribution for the Primakoff reaction:

1. Two p_T^2 regions were defined (Fig. 5, upper right), one at $p_T^2 < 0.001 \text{ GeV}^2/c^2$ where the Primakoff effect dominates, and one at $0.002 < p_T^2 < 0.006 \text{ GeV}^2/c^2$ for estimation of the background from coherent production of the $\Lambda\pi$ system. The corresponding mass spectra are shown in Fig. 5, center left. Subtraction yields the data points in Fig. 5, center right and lower left.
2. All events were subdivided into 20 MeV bins of the mass spectrum of the final $\Lambda\pi$ state, and the p_T^2 distribution analyzed for each bin. The result is shown as the shaded histogram in Fig. 5, center right and lower right.

Both methods are in reasonable agreement (Fig. 5, center right). The total cross section for the process is given by the equation

$$\sigma_{tot} = \int_0^\infty \frac{d\sigma}{dt} dt = A \cdot \Gamma(\Sigma(1385)^- \rightarrow \Sigma^-\gamma).$$

A was obtained by integrating numerically over the differential cross section $d\sigma/dt$. The radiative width $\Gamma(\Sigma(1385)^- \rightarrow \Sigma^-\gamma)$ was estimated using the expression

$$\Gamma(\Sigma(1385)^- \rightarrow \Sigma^-\gamma) = \frac{N_{\Sigma^*}}{A \cdot L \cdot \epsilon \cdot \text{BR}(\Sigma^* \rightarrow \Lambda\pi) \cdot \text{BR}(\Lambda \rightarrow p\pi)},$$

where N_{Σ^*} is the number of observed events, L the luminosity of the experiment, ϵ the combined reconstruction efficiency where efficiency of the applied cuts and finite decay volume have been accounted for. The luminosity was determined on the basis of coherent production of $(\pi^-\pi^-\pi^+)$ by pions [29].

The upper limit for the Primakoff production of $\Sigma(1385)^-$ is: $N_{\Sigma^*} < 205$ events at 95 % confidence limit. With the above equation this yields

$$\Gamma(\Sigma(1385)^- \rightarrow \Sigma^-\gamma) < 12 \text{ keV (95 \% CL)},$$

thus improving the upper limit of 24 keV established by an experiment at Brookhaven (1977) [31].

V CONCLUSIONS

A measurement of the Σ^- mean squared charge radius has been performed by elastic Σ^- -electron scattering. A preliminary analysis yields a Σ^- radius of $\langle r^2 \rangle_{\Sigma^-} = 0.60 \pm 0.08$ (*stat.*) ± 0.08 (*syst.*) fm². The π^- radius was determined in parallel and is found to be in excellent agreement with previous experiments.

The Σ^- p total hadronic cross section has been measured at 600 GeV/c. We obtain $\sigma_{tot}(\Sigma^-p) = 34.0 \pm 1.9$ mb from the difference of results for CH₂ and C targets, and $\sigma_{tot}(\Sigma^-p) = 36.6 \pm 0.9$ mb from a Glauber model calculation using the ratios of Σ^- A to pA cross sections on C and Be targets.

A new upper limit for the radiative width of the $\Sigma(1385)^-$ has been established at 12 keV (95 % CL) from a study of Primakoff production on lead nuclei.

Improved statistics and smaller systematic errors for these results as well as other hyperon physics results are expected as the analysis of SELEX data proceeds.

ACKNOWLEDGEMENTS

We are indebted to B. C. LaVoy, D. Northacker, F. Pearsall, and J. Zimmer for invaluable technical support. This project was supported in part by Bundesministerium für Bildung, Wissenschaft, Forschung und Technologie, Consejo Nacional de Ciencia y Tecnología (CONACyT), Conselho Nacional de Desenvolvimento Científico e Tecnológico, Fondo de Apoyo a la Investigación (UASLP), Fundação de Amparo à Pesquisa do Estado de São Paulo (FAPESP), the Israel Science Foundation founded by the Israel Academy of Sciences and Humanities, Istituto Nazionale de Fisica Nucleare (INFN), the International Science Foundation (ISF), the National Science Foundation (Phy #9602178), NATO (grant CR6.941058-1360/94), the Russian Academy of Science, the Russian Ministry of Science and Technology, the Turkish Scientific and Technological Research Board (TÜBİTAK), the U.S. Department of Energy (DOE grant DE-FG02-91ER40664), and the U.S.-Israel Binational Science Foundation (BSF).

REFERENCES

1. A. Kushnirenko, these proceedings.
2. V. Kubarovsky, "Radiative width of the a_2 meson", presented at the XXIX International Conference on High-Energy Physics, Vancouver, July 23-29, 1998.
3. B. Povh and J. Hüfner, *Phys. Lett. B* **245**, 653 (1990).
4. I. Eschrich, *Measurement of the Σ^- Charge Radius at the Fermilab Hyperon Beam*, MPIH-V22-1998, Ph.D. thesis, MPI f. Kernphysik / Univ. Heidelberg, 1998.
5. M. Adamovich et al., *First observation of Σ^- -e scattering in the hyperon beam experiment WA89 at CERN*, submitted to *Eur. Phys. J. C*, (1998).
6. K. Vorwalter, *Determination of the Pion Charge Radius with a Silicon Microstrip Detector System*, MPIH-V23-1998, Ph.D. thesis, MPI f. Kernphysik / Univ. Heidelberg, 1998.
7. S. Amendolia et al., *Nucl. Phys. B* **277**, 186 (1986)
8. B. V. Geshkenbein, *hep-ph/9806418* (1998).
9. G. Simon, C. Schmitt, F. Borkowski, and V. Walther, *Nucl. Phys. A* **333**, 381 (1980)
10. L. Hand, D. Miller, and R. Wilson, *Rev Mod Phys* **35**, 335 (1963)
11. J. Murphy, Y. Shin, and D. Skopik, *Phys. Rev. C* **9**, 2125 (1974)
12. P. Mergell, U. Meissner, and D. Drechsel, *Nucl. Phys. A* **596**, 367 (1996)
13. T. Udem et al., *Phys. Rev. Lett.* **79**, 2646 (1997)
14. J. Kunz, P. Mulders, and G. Miller, *Phys. Lett. B* **255**, 11 (1991)
15. N. Park and H. Weigel, *Nucl. Phys. A* **541**, 453 (1992)
16. S. Sahu, *Mod. Phys. Lett. A* **10**, 2103 (1995)
17. H. Kim, A. Blotz, M. Polyakov, and K. Goeke, *Phys. Rev. D* **53**, 4013 (1996)
18. G. Wagner, A. Buchmann, and A. Faessler, *nucl-th/9809015*, accepted for publication by *Phys. Rev. C*, (1998).
19. A. Donnachie and P.V. Landshoff, *Phys. Lett. B* **296**, 227 (1992)
20. H1 Collaboration, *Z. Phys. C* **69**, 27 (1995).
21. ZEUS Collaboration, *Phys. Lett. B* **350**, 120 (1995).
22. WA42 Collaboration (Biagi *et al.*), *Nucl. Phys. B* **186**, 1 (1981).
23. B. Kopeliovich, private communications.
24. A. Levy, *Soft Interactions at High Energy*, DESY Report 95-204.
25. U. Dersch, *Messung totaler Wirkungsquerschnitte mit Σ^- , p, π^- und π^+ bei 600 GeV/c Laborimpuls*, Ph.D. thesis (*in German*), MPI f. Kernphysik / Univ. Heidelberg, 1998.
26. Particle Data Group, *Phys. Rev. D* **54**, 1 (1996).
27. J. Badier *et al.*, *Phys. Lett. B* **41**, No. 3, 387 (1972).
28. L.G. Landsberg and V.V. Molchanov, *Radiative Decays of Hyperons*, IHEP 97-42, Protvino 1997 and references herein;
H.J. Lipkin and M.A. Moinester, *Phys. Lett. B* **287**, 179 (1992);
G. Wagner *et al.*, *Phys. Rev. C* **58**, No. 3, 1745 (1998).
29. M. Zielinski *et al.*, *Z. Phys. C* **16**, 197 (1983)
30. V. Kubarovsky, *Upper Limit for the Radiative Width of $\Sigma(1385)^-$ and Photoproduction Cross Section for the Reaction $\gamma + \Sigma^- \rightarrow \pi^- + \Lambda$* , H-Note 809 (SELEX Internal Report), 1998.

31. E. Arik *et al.*, *Phys. Rev. Lett.* **38**, No. 18, 1000 (1977).